JOURNAL OF APPLIED ELECTROCHEMISTRY 24 (1994) 639–646

An experimental study of the frequency response of electrochemical sensors in nonhomogeneous flow in packed beds

S. RODE, M. A. LATIFI, A. STORCK, N. MIDOUX

Laboratoire des Sciences du Génie Chimique, CNRS–ENSIC, BP-451, 1-rue Grandville, 54001 Nancy Cedex, France

Received 10 May 1993; revised 12 September 1993

Circular electrochemical probes were mounted flush with the wall of a packed bed operating either in single-phase liquid flow or in gas–liquid downflow. Frequency analysis of the measured diffusion current indicated that the recently determined mass transfer function of the probes is approximately valid, even under spatially nonhomogeneous flow conditions, provided that the relative fluctuation intensity of the current does not exceed 0.15. Correction of the current measurements in the frequency domain by means of the mass transfer function was necessary in order to determine the fluctuating characteristics of the velocity gradient.

List of symbols

C_∞	bulk concentration of the reacting species (mol m^{-3})
D	diffusion coefficient of the reacting species (m^2 s^{-1})
d	probe diameter (m)
d_p	particle diameter (m)
F	Faraday number ($F = 96\,500$ C equiv^{-1})
G	superficial gas flow rate (kg m^{-2} s^{-1})
f	frequency (s^{-1})
$H(f), H'(f), H(\sigma)$	dimensional and dimensionless probe transfer functions
$\|H(0)\|$	quasi steady state solution of $H(f) = 1/3\bar{I}/\bar{S}$ (A s)
I	instantaneous diffusion current (A)
i	fluctuating component of the diffusion current, $I - \bar{I}$ (A)
L	superficial liquid flow rate (kg m^{-2} s^{-1})
Re	liquid Reynolds number $= L\, d_p/\mu_L$ as defined by Equation 2(–)
S	instantaneous velocity gradient (s^{-1})
s	fluctuating component of the velocity gradient, $S - \bar{S}$ (s^{-1})
t	time (s)
T_i, T_s	fluctuation intensity of the diffusion current and the velocity gradient (–)
$W_{ii}(f), W'_{ii}(f)$	power spectral density functions of the diffusion current
$W_{ss}(f), W'_{ss}(f)$	power spectral density functions of the velocity gradient

Greek symbols

ν_e	number of electrons involved (–)
γ	dimensionless amplitude of the velocity gradient modulation (–)
μ_L	liquid viscosity (kg m^{-1} s^{-1})
σ	dimensionless frequency defined by Equation 4 (–)
τ	relaxation time of the mass transfer boundary layer Equation 5 (s)

Superscripts

$\bar{\ }$	average value
$\|\ \|$	amplitude of a complex function

1. Introduction

A major drawback of the use of electrochemical probes in the study of hydrodynamics is their poor frequency response, which is due to the low value of the molecular diffusion coefficient in liquids. This problem has been partially solved by Nakoryakov *et al.* [1, 2] and Deslouis *et al.* [3, 4] who calculated the transfer function of rectangular and circular probes; the latter also proceeded to an experimental verification. Both the computation and the experiments were made assuming spatially homogeneous flow and in conditions where the fluctuating part of the mass balance

This paper was presented at the International Workshop on Electrodiffusion Diagnostics of Flows held in Dourdan, France, May 1993.

0021-891X

equation could be described by a linear approximation. The limits of the use of this transfer function have not been yet experimentally tested, and it was interesting to know whether it could be applied in nonhomogeneous flow conditions. In the present work, a network of 25 small circular electrochemical probes was mounted flush with the wall of a packed bed reactor operating either in single-phase liquid flow or in gas–liquid downflow. The local flow was nonhomogeneous in space and gave high frequency fluctuations. In this paper we focus on the frequency analysis of the diffusion current measurements. Other experimental results are given in [5, 6] and [7].

2. Theory

2.1. *Time averaged response of circular sensors*

In the following we will discuss the case of a circular probe embedded flush with a solid wall over which a liquid is flowing, forming a hydrodynamic boundary layer. The thickness of the diffusion boundary layer is considered to be small compared to the electrode diameter. Molecular diffusion in the direction of the mean flow and in the transverse direction can consequently be neglected in comparison to diffusion normal to the solid surface. Numerical solutions of the mass balance equation [8] suggest that this condition is fulfilled for $Sd^2/D > 1600$ where S is the velocity gradient in the flow direction, d the probe diameter and D the diffusion coefficient of the reacting species. We also assume that the mean flow and its fluctuations are homogeneous in space over the sensor at any instant. Under these conditions, and considering situations where the time dependent velocity gradient fluctuations are much lower than the average velocity gradient, the average diffusion current, $\bar{I}$, delivered by the probes and the average velocity gradient in the flow direction, $\bar{S}$, at the probe surface are related by [9]:

$$\bar{I} = 0.677 \nu_e F C_\infty D^{2/3} d^{5/3} \bar{S}^{1/3} \tag{1}$$

where ν_e is the number of electrons involved, F the Faraday number, and C_∞ the bulk concentration of the reacting species. Considering the circular geometry of the probes, the mean direction of the flow in the plane of the solid wall is immaterial and may even change.

Recent literature results show that the average current response of circular electrochemical probes is, in fact, quite insensitive to flow nonuniformity [10], and to high amplitude fluctuations of the velocity gradient [11]. The influence of the latter can, moreover, be easily corrected [6] and the average velocity gradient can be evaluated approximately by

$$\bar{S} \simeq a\bar{I}^3(1 + 3T_i^2) \tag{2}$$

where a is given by Equation 1 and T_i is the fluctuating intensity of the diffusion current: $T_i = \sqrt{(\overline{i^2})}/\bar{I}$. The fluctuating component of the instantaneous diffusion current, i, is given by $i = I - \bar{I}$.

Assuming nonreversing boundary layer flow, circular electrochemical probes can consequently be used even in extremely nonhomogeneous and fluctuating flows to measure the average local velocity gradient at the liquid–solid interface.

2.2. *Frequency response of the sensors*

In unsteady flows the time variation of the velocity gradient causes a time variation of the diffusion current. Like any physical system, the mass transfer process in the diffusion layer takes a finite time, and the diffusion layer acts as a high frequency filter of the velocity gradient fluctuations. Owing to the low value of the molecular diffusion coefficient in liquids, the cutoff frequency of this filter is rather low and hence a detailed knowledge of its characteristics beyond the cutoff frequency is necessary to interpret instantaneous measurements accurately.

2.2.1. Case of low amplitude fluctuations: the linear approximation. If the fluctuations of the instantaneous diffusion current are much lower than the average diffusion current, the behaviour of the probe filter may be discussed within the framework of a linear theory. Assuming the velocity gradient fluctuations as random and the system as steady from a statistical point of view, the power spectral density (p.s.d.) of the diffusion current $W_{ii}(f)$ and that of the velocity gradient $W_{ss}(f)$ are then linked through the following relationship [3]:

$$W_{ii}(f) = |H(f)|^2 W_{ss}(f) \tag{3}$$

where $|H(f)|$ is the amplitude of the mass transfer function $H(f)$.

For the theoretical calculation of the transfer function of electrochemical sensors, the frequencies are normalized with respect to the relaxation time of the mass transfer boundary layer above the probe, τ:

$$\sigma = 2\pi f \tau \tag{4}$$

where

$$\tau = \left(\frac{d^2}{D\bar{S}^2}\right)^{1/3} \tag{5}$$

$H(\sigma)$ has been recently determined by Nakoryakov *et al.* [1, 2] and Deslouis *et al.* [3, 4], who proceeded additionally to an experimental verification. The results given by these authors are in good agreement. For $\sigma \leqslant 1$ the velocity gradient fluctuations are slow compared with the characteristic time response of the system. Equation 1 is valid at each instant and the amplitude of the transfer function does not depend on the frequency, this is referred to as the quasi-steady state solution: $|H(0)| = 1/3\bar{I}/\bar{S}$. For $\sigma > 1$ $|H(\sigma)|$ depends on the dimensionless frequency. Pertinent expressions are given in [1] and [3].

2.2.2. Case of large amplitude fluctuations – limits of the linear approximation. Kaiping [11], and Mao and Hanratty [12, 13] studied the behaviour of

electrochemical probes in flow with large amplitude oscillations. The experiments and the numerical computations were made for sine wave modulated flow over rectangular probes but may be transposed to circular probes. The dimensionless amplitude of the velocity gradient fluctuations, γ, was defined as the ratio of the amplitude of the sine wave modulation to the average velocity gradient. We only consider here the results obtained for nonreversing flow which means that $\gamma \leqslant 1$. Kaiping [11] and Mao and Hanratty [13] solved numerically the mass balance equation for $\gamma = 0.5$ and $\gamma = 0.9$. According to these results, summarized in [6], the linear approximation holds quite well for $\gamma = 0.5$. Experiments performed by Mao and Hanratty in pipe flow [12] with γ reaching values up to 0.6 were also found in good agreement with the predictions of the linear theory. For $\gamma = 0.9$, the response of the mass transfer layer to a sine wave flow modulation is no longer of sinusoidal shape [11, 13]: the distortion by inertial effects is much more discernible at the minimum, where convection is small and inertia is significant than at the maximum, where convection dominates and the influence of inertia is comparatively small, Kaiping reported a small distortion, even for $\gamma = 0.5$. These phenomena cannot be detected by linear theory.

In hydrodynamic systems, velocity gradient fluctuations are generally random and a very simple way to evaluate their relative amplitude is to calculate the fluctuating intensity: $T_s = (\sqrt{(\overline{s^2})}/\bar{S})$. Considering the fluctuating intensity of a sine wave modulated flow ($T_s = 0.707\gamma$), the linear approximation holds for $T_s = 0.35$ and approximately even for $T_s = 0.42$. It does not hold anymore for $T_s = 0.64$. In the quasi steady-state domain, according to Equation 2, the fluctuating intensity of the velocity gradient is related to that of the diffusion current by

$$T_s \simeq \frac{3T_i}{1 + 3T_i^2} \tag{6}$$

The linear approximation holds then approximately for $T_i = 0.12$ and even for $T_i = 0.15$ [12]. It is not valid anymore for $T_i = 0.25$.

3. Experiments

3.1. *Experimental setup and investigated domain*

Local velocity gradient measurements were made by means of circular electrochemical probes mounted flush with the wall of a packed bed reactor operating either in single or two phase flow.

3.1.1. Experimental rig. The reactor was a glass column with an inside diameter of 50 mm, packed with 5 mm glass spheres; its height was 1.3 m. Electrolyte solution was fed to the reactor from a storage tank by means of a centrifugal pump. The electrolyte temperature was maintained at 30°. The gas phase, nitrogen, was delivered by a gas distribution network. The bed voidage, defined as the ratio of the volume accessible to the fluid phases to the overall bed volume was 0.4. In single phase flow the bed voidage was entirely filled with the liquid phase, whereas in two phase flow it was partly occupied by the gas phase. The relative occurrence of the two phases in the bed voidage was then a function of the gas and liquid flow rates. More details and a schematic drawing of the experimental apparatus are given in [5–7].

The liquid was an aqueous solution of 0.003 M potassium ferricyanide, 0.02 M potassium ferrocyanide and 0.5 M sodium hydroxide as a supporting electrolyte. The test reaction was the reduction of ferricyanide ions. Their bulk concentration was determined before each experiment by spectrophotometry. Analytical grade ferri- and ferrocyanides were used and no solution was kept more than four days. The diffusion coefficient of ferricyanide was taken from Hiraoka *et al.* [14], as $7.42 \times 10^{-10}\,m^2\,s^{-1}$; the values of the viscosity and the density of the solution were $0.928 \times 10^{-3}\,kg\,m^{-1}\,s^{-1}$ and $1020\,kg\,m^{-3}$ respectively.

3.1.2. Measuring system. The measuring system consisted of an array of 25 circular platinum electrochemical probes, mounted flush with the wall of the reactor. They were set out on a 5 mm × 5 mm square array and each of them could act as a working electrode. The counter electrode was a nickel cylinder constituting part of the column wall and located downstream. Four probes were polarized simultaneously on the diffusion plateau of the cathodic reaction (−0.4 V) and the potentials delivered by the current–voltage converter (analogous to the converter shown in [9]) were sampled at 512 Hz in single phase flow and at 1024 Hz in two phase flow. The sampling time was 250 s, the signals were stored on the hard disk of a HP 9000/360 computer.

Great attention was given to the calibration of the probes. Their diameters were determined by two independent methods: electrochemical measurements in the empty column and photographs of the element. The results of the two methods were in good agreement, the 19 working probes (six probes gave unsatisfactory results) had approximately the same diameter: 287 μm with a standard-deviation of 2%.

3.1.3. Investigated flow regimes. The results presented were obtained for single phase flow in the 'chaotic' flow regime, observed for Reynolds numbers above 150, and for two-phase flow in the dispersed bubble flow regime, where the liquid is the continuous phase and the gas passes down the bed in the form of elongated bubbles. In both flow regimes the probe currents gave high frequency fluctuations. The fluctuation intensity, T_i, was lower than 0.12 for almost all the measurements made in single phase flow and for some of the measurements made in two-phase flow; these measurements could be treated in the framework of a linear theory.

3.1.4. Calculation procedure of the power spectral densities (p.s.d.). The p.s.d. of the diffusion current $W_{ii}(f)$ were calculated by the product of the discrete frequency spectrum of the sampled signal, obtained by Fourier transform, with its conjugate. These elementary p.s.d., calculated over 8 s in an effective frequency range from 0.125 to 205 Hz or 0.125 to 409 Hz, were averaged with a time overlap of 80%. The estimation error of the resulting p.s.d., an average value of 148 elementary p.s.d., was about 8%. The shape of $W_{ss}(f)$ was obtained by dividing $W_{ii}(f)$ by the normalized transfer function $|H(f)|^2/|H(0)|^2$ evaluated using Equations 1 and 3 and the expressions of $|H(\sigma)|$ given in [3]. For low frequencies, in the quasisteady state domain, the normalized transfer function equals 1 and $W_{ii}(f)$ and $W_{ss}(f)$ took the same value and were superimposed on the plots. On all our plots, $W_{ii}(f)$ and $W_{ss}(f)$ are given in V^2s, as the signals delivered by the current–voltage converter.

3.2. *Evaluation of the spatial nonhomogeneity of the flow*

The difference between the average velocity gradients measured on different probes of the network at a given liquid (or gas and liquid) flow rate may be due to flow nonhomogeneity in the pore space but also to experimental errors. Reproducibility tests indicated that the standard deviation of the local mass transfer rate (depending on $\bar{I}$ and C_∞^{-1}) was 3.5% for a given probe and given gas and liquid flow rates. The precision of the probe diameter being 2% (standard deviation) and considering that the local velocity gradient depends on $\bar{I}^3$, C_∞^{-3} and d^5 (see Equation 1), the estimation error of the latter was at least of about 20% (standard deviation).

Figures 1 and 2 present examples of average measurements performed on 18 working probes for single and two phase flow, respectively. The arrows indicate the overall, and the most probable, local flow directions. We also represented the approximate position of the glass sphere touching the reactor wall. As can be seen, probes very close to, or immediately below, a solid–solid contact point (which is at the centre of the circle) had very low velocity gradients, the fluid flow passing round and avoiding the latter. The overall flow was quite nonhomogeneous in single-phase flow and quite homogeneous in two phase flow experiments (except for the probes placed very close to a solid–solid contact point where it was also nonhomogeneous in two-phase experiments).

In single phase flow, considering the average probe diameter (287 μm), the distance between two probes (1250 μm), as well as the great difference often observed between the velocity gradients determined on two neighbouring probes (see Fig. 1), it is quite probable that the average flow was not always homogeneous at the probe scale. As shown by Wein and Sobolik [10], this nonuniformity does not really matter for the applicability of Equation 1 which then evaluates the average velocity gradient at the

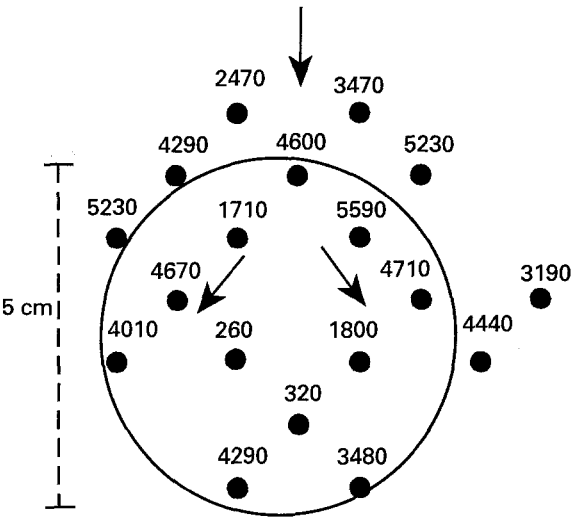

Fig. 2. Example of the average local velocity gradients measured on the different probes in two-phase flow ($L = 27.1\,kg\,m^{-2}\,s^{-1}$; $G = 0.054\,kg\,m^{-2}\,s^{-1}$).

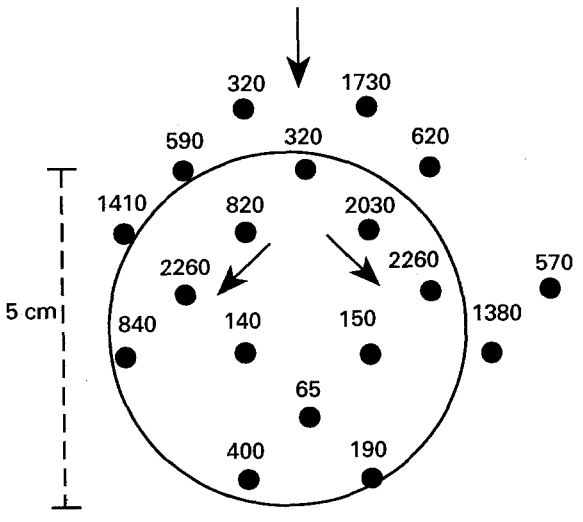

Fig. 1. Example of the average local velocity gradients measured on the different probes in single phase flow ($L = 56.1\,kg\,m^{-2}\,s^{-1}$; $Re = 303$).

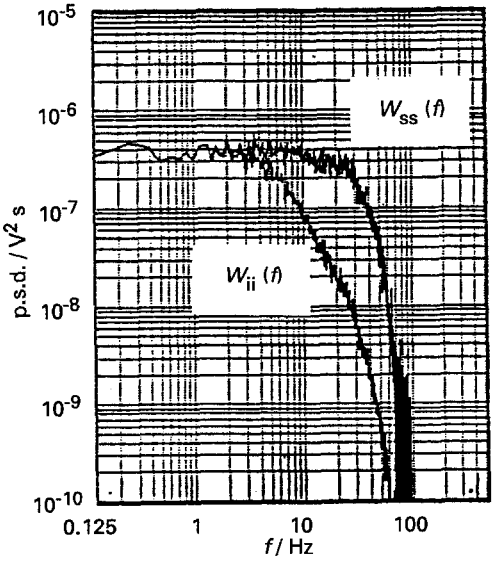

Fig. 3. Typical shapes of the p.s.d.'s in single phase flow ($Re = 303$; $T_i = 0.11$; $\bar{S} = 320\,s^{-1}$).

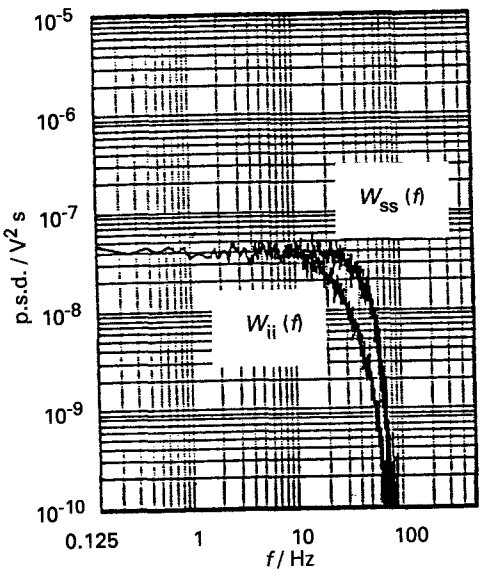

Fig. 4. Typical shapes of the p.s.d.'s in single phase flow. ($Re = 303$; $T_i = 0.03$; $\bar{S} = 2260\,s^{-1}$).

probe centre; but we were not sure whether it would influence the instantaneous behaviour of the velocity gradient and whether the expressions of the transfer function, given in [1] and [3], were still valid.

3.3. *Frequency analysis in single phase flow*

3.3.1. Shape of most of the power spectral densities and interpretations. Two examples of the calculated and the corrected power spectral densities for a Reynolds number of 303 and for well exposed probes are given on Figs 3 and 4. The applied transfer function gave consistent results and the overall shape of $W_{ii}(f)$ and $W_{ss}(f)$, being almost the same for all measurements made at Reynolds numbers higher than 170, was characteristic for random steady state fluctuations of the velocity gradient (see [15]). For low frequencies the spectra were flat, corresponding to white noise and, after the cutoff frequency of the considered system, the power was a decreasing function of frequency. The flat part of $W_{ii}(f)$ was always less extensive than the flat part of $W_{ss}(f)$; this signifies that the mass transfer cutoff frequency of the diffusion layer above the probes f_M was always lower than the hydrodynamic cutoff frequency of the velocity gradient fluctuations f_H; the fluctuations of the time-dependent diffusion current were consequently greatly influenced by the time-response of the diffusion layer.

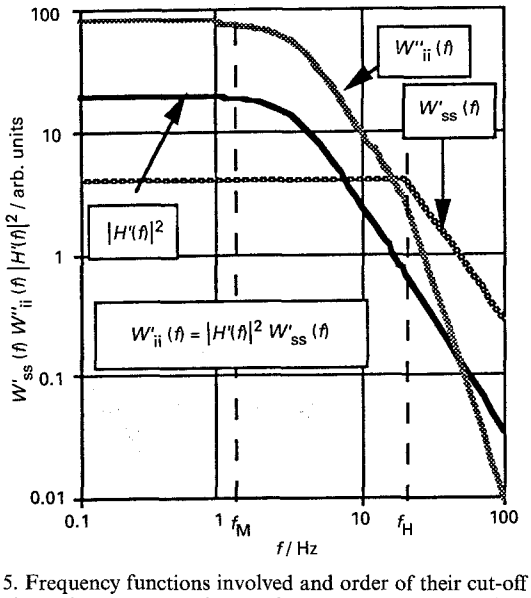

Fig. 5. Frequency functions involved and order of their cut-off frequencies. (f_M: mass transfer cutoff frequency; f_H: hydrodynamic cutoff frequency).

Figure 5 presents schematically the different frequency functions involved (designed by $W'_{ii}(f)$, $|H'(f)|^2$ and $W'_{ss}(f)$) and the order of their cutoff frequencies; the power spectral density axis and the frequency axis are in arbitrary units on this plot. For greater clarity, and unlike all the other presented spectra, the transfer function was chosen to be not unity in the quasi-steady state domain (we chose a value of 20) and $W'_{ii}(f)$ and $W'_{ss}(f)$ are consequently not superimposed. We indicated on this plot the localization and the order of the cut-off frequencies of the different functions, defined as the frequency value where the spectra are no longer flat but start to decrease with increase in frequency.

Comparison of Figs 3 and 4 clearly demonstrates the importance of frequency analysis in the investigations on flow hydrodynamics. The frequency behaviour of the diffusion current, which can be seen on the shape of $W_{ii}(f)$, is very different for the two measurements. Compared with Fig. 4 the fluctuating velocity gradient signal was much more damped in the case presented in Fig. 3, where the average velocity gradient on the probe was seven times less than that of the measurement presented in Fig. 4. On the contrary, the frequency behaviour of the instantaneous velocity gradient, which can be seen on the shape of $W_{ss}(f)$, was close for both measurements.

The fluctuation intensities of the diffusional current, T_i, were very different for the measurements presented on Figs 3 and 4 (0.11 and 0.03, respectively). In the quasisteady state domain, the fluctuation intensity of the velocity gradient, T_s, is about three times that of the diffusional current and may be evaluated by Equation 6. Considering the fact that our measurements were additionally damped by the probe transfer function the relationship is no longer so simple and we did not try to evaluate the corresponding T_s values. These seemed to be quite different for the measurements made on different probes.

3.3.2. Some strange shapes of the power spectral densities. At all liquid flow rates, the measurements made on certain probes exhibited a change in slope of $W_{ii}(f)$ in the high frequency range. $W_{ss}(f)$ then gave a second 'plateau' in the high frequency domain. An example is given in Fig. 6. This phenomenon has not yet been explained.

Some of the power spectral densities of the velocity gradient $W_{ss}(f)$ were not perfectly flat before the

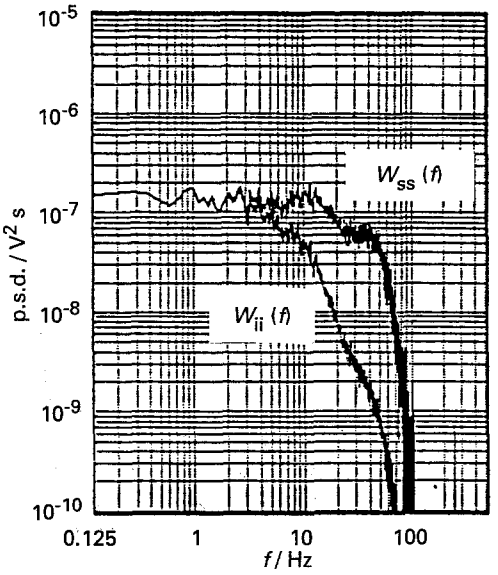

Fig. 6. P.s.d.'s presenting a second 'plateau'. ($Re = 303$; $T_i = 0.07$; $\bar{S} = 400\,s^{-1}$).

hydrodynamic cutoff frequency, but exhibited peak values; an example is given in Fig. 7. This strange shape might be due to hydrodynamic particularities of the local flow but could as well be due to the uncertainty of the calculations. Considering the estimation errors of the diffusional current and the probe diameter (see Section 3.2), the estimation accuracy of σ is not better than 15% (standard deviation). The resulting estimation error on $|H(f)|^2$ could reach up to 50% and it is consequently not surprising to find some unusual shapes among the corrected spectra. Further investigations are needed to better understand the reasons for the observed anomalies.

3.4. *Frequency analysis in two phase flow*

In two phase flow, and for given gas and liquid flow rates, the average local shear rate was quite homogeneous all over the pore space (see also Fig. 2),

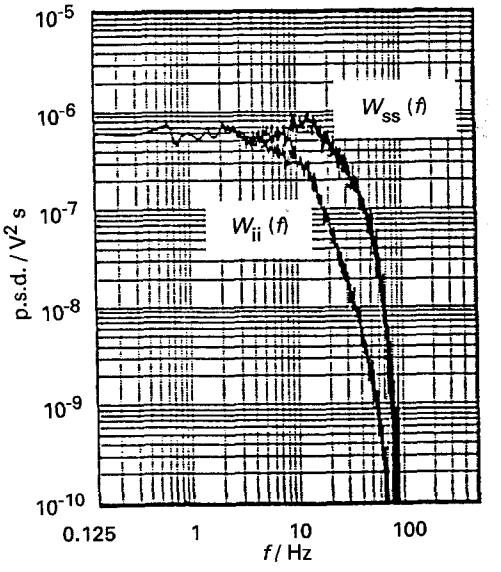

Fig. 7. P.s.d.'s presenting a peak value. ($Re = 303$; $T_i = 0.14$; $\bar{S} = 590\,s^{-1}$).

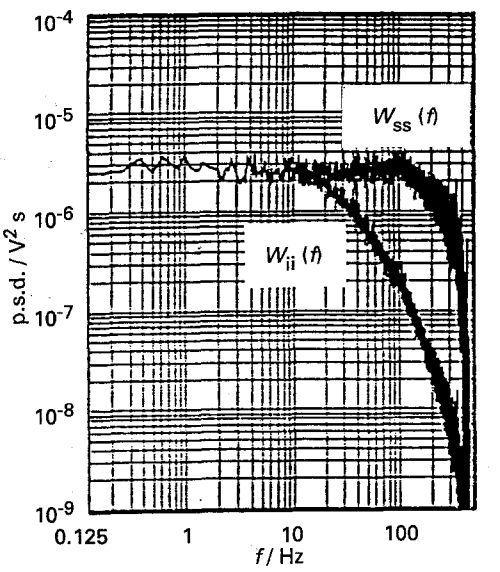

Fig. 8. Typical shapes of the p.s.d.'s in two-phase flow: linearity conditions satisfied. ($L = 27.1\,kg\,m^{-2}\,s^{-1}$; $G = 0.054\,kg\,m^{-2}\,s^{-1}$); $T_i = 0.10$; $\bar{S} = 3100\,s^{-1}$.

except for probes located very close to a solid–solid contact point. The fluctuation intensity of the diffusion current was much more significant than in single-phase flow and most of the measurements could not be treated in the framework of a linear theory. For some gas and liquid flow rates the linearity conditions were nevertheless approximately satisfied; two examples of such measurements are presented in Figs 8 and 9. The situation was similar to that described in single phase flow: the shapes of $W_{ii}(f)$ and $W_{ss}(f)$ were characteristic of random steady state fluctuations of the velocity gradient and the transfer function was approximately valid. As in single phase flow measurements, the mass transfer cutoff frequency, f_M, was always lower than the hydrodynamic cutoff frequency of the velocity gradient fluctuations, f_H. The distance between f_M and f_H was much more pronounced.

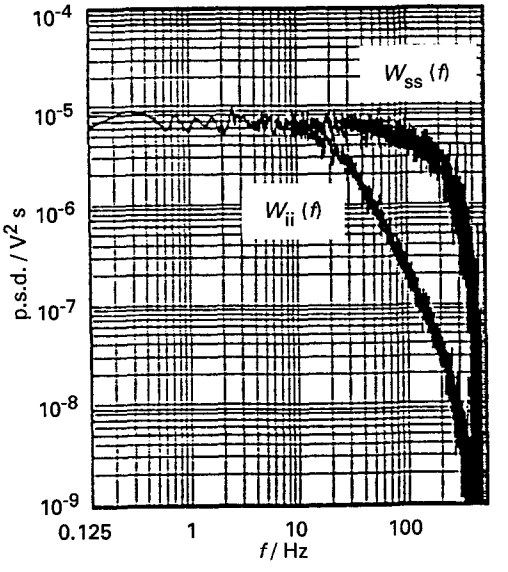

Fig. 9. Typical shapes of the p.s.d.'s in two-phase flow: linearity conditions satisfied. ($L = 27.1\,kg\,m^{-2}\,s^{-1}$; $G = 0.032\,kg\,m^{-2}\,s^{-1}$; $T_i = 0.15$; $\bar{S} = 2310\,s^{-1}$).

Figures 4 and 9 were made for measurements with almost the same average velocity gradient. Consequently the mass transfer cutoff frequencies of the two measurements, influencing the frequency behaviour of $W_{ii}(f)$, were very close, even though their hydrodynamic cutoff frequencies, which can be seen on the shape of $W_{ss}(f)$, were very different. Once again the correct interpretation of hydrodynamic fluctuations was only possible after correction with the transfer function of the probes.

An example of $W_{ii}(f)$ and $W_{ss}(f)$, calculated for high fluctuation intensities, is given in Fig. 10. The p.s.d. did not present any 'flat part' and the frequency analysis did not make much sense.

3.5. *Influence of the probe diameter*

3.5.1. Theoretical considerations. In two phase flow the ratio between the mass-transfer and the hydrodynamic cutoff frequencies was about 10 for probes with a diameter of 287 μm. Considering that, for a given velocity gradient, the dimensionless frequency σ is proportional to $d^{2/3}$ (Equations 4 and 5), the probe diameter required to have the two cutoff frequencies of the same order of magnitude would be 9 μm. With a probe of this diameter, considering the values of $\bar{S}$ measured, the diffusion in the direction of the mean flow and in the transverse direction could no longer be neglected and Equation 1 could not be applied. To measure the velocity gradient under the present flow conditions, electrochemical probes have consequently to be larger than 9 μm and instantaneous velocity gradient measurements must always be corrected in the frequency domain.

3.5.2. Experiments. In order to test the influence of the probe diameter on the experimental results, some probes were manufactured with a diameter of about 140 μm. The manufacturing and calibration of these probes was difficult and the precision on the probe-diameter was not very good (10% standard deviation). The diffusion current being quite small (it is proportional to $d^{5/3}$, see Equation 1), the experimental error on its determination was much greater than that for larger probes. Additionally, the signal being less filtered than on the larger probes, T_i was always higher than 0.15 which is the limit of the validity of the linear approximations (see Section 2.2).

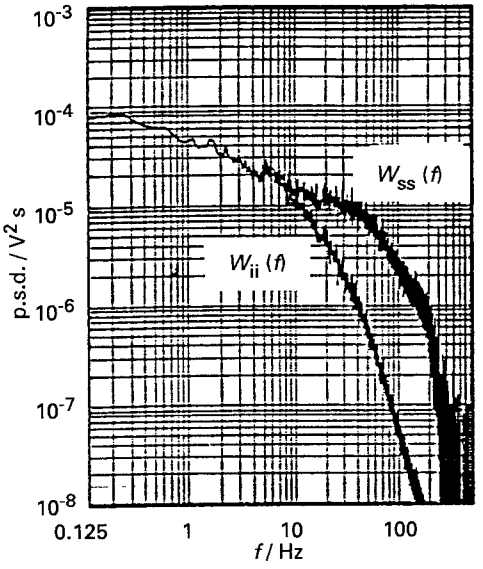

Fig. 10. Typical shapes of the p.s.d.'s in two-phase flow: linearity conditions not satisfied: ($L = 13.4\,\mathrm{kg\,m^{-2}\,s^{-1}}$; $G = 0.032\,\mathrm{kg\,m^{-2}\,s^{-1}}$; $T_i = 0.25$; $\bar{S} = 1370\,\mathrm{s^{-1}}$).

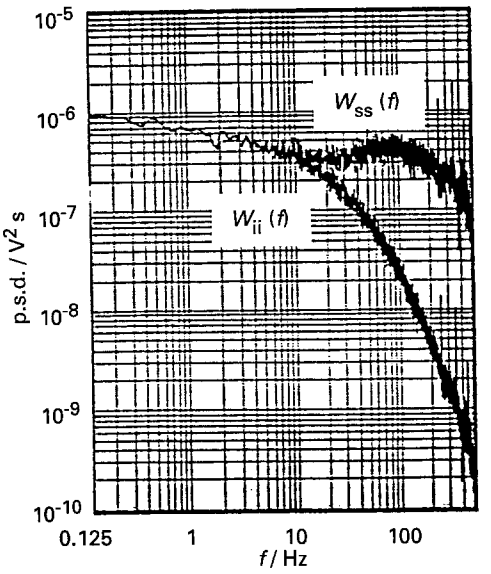

Fig. 11. P.s.d.'s measured in two phase flow on a small probe; $d = 140\,\mu$m. ($L = 27.1\,\mathrm{kg\,m^{-2}\,s^{-1}}$; $G = 0.054\,\mathrm{kg\,m^{-2}\,s^{-1}}$; $T_i = 0.16$; $\bar{S} = 1200\,\mathrm{s^{-1}}$).

Figure 11 presents a p.s.d. measurement with its correction made on one of these probes. We cannot observe a real 'plateau' on the shape of $W_{ii}(f)$ and the shape of $W_{ss}(f)$ is quite strange. This might be due to the significant estimation error on the average velocity gradient (the standard deviation of which was easily greater than 50%) inducing a significant error in the estimation of the dimensionless frequency and, consequently, on the corrected p.s.d. of the velocity gradient. It can nevertheless be seen that, as predicted by the theoretical considerations, the instantaneous diffusion current is still strongly influenced by the transfer function. The use of probes with smaller diameters strongly increases the manufacturing difficulties and the experimental errors without a great improvement in the frequency response.

4. Conclusion

Even though the average flow was, in single phase flow, nonhomogeneous in space, the transfer function of the electrochemical probes given in the literature [1, 3] seemed to be approximately valid for $T_i < 0.15$. This is in good agreement with the limits of the linear assumptions, as found in the literature by numerical simulations [11, 13]. It constitutes an experimental confirmation of the validity-domain of the transfer function. The analysis of the power spectral density functions of the velocity gradient $W_{ss}(f)$, enabled us to determine, via the autocorre-

lation function, characteristic time and length scales of the flow fluctuations in single and in two-phase flow [6, 7]. The characteristic length-scale was found to be the pore space and, consequently, flow fluctuations seemed to be homogeneous in space over the probes at any instant and this might also be a reason why the probe transfer function worked. The signal being strongly damped by the mass-transfer function, especially in two-phase flow, the error on the frequency behaviour of $W_{ss}(f)$ may be significant and only order of magnitude analysis may be made with these functions.

Acknowledgement

The authors are grateful to C. Deslouis and B. Tribollet (LP 15 du CNRS Physique des Liquides et Electrochimie, Paris) for helpful suggestions, as well as to the Institut Français du Pétrole for financial support.

References

[1] V. E. Nakoryakov, O. N. Kashinsky and B. K. Kozmenko, *in* IUTAM Symposium, Nancy, France (1983) p. 695.
[2] V. E. Nakoryakov, A. P. Budukov, O. N. Kashinsky and P. I. Geshev, 'Electrodiffusion Method of Investigation into Local Structure of Turbulent Flows', (edited by V. G. Gasenko), Novosibirsk, in Russian (1986).
[3] C. Deslouis, O. Gil and B. Tribollet, *J. Fluid Mech.* **215** (1990) 85.
[4] *Idem, Int. J. Heat Mass Transfer* **33** (1990) 2525.
[5] S. Rode, Thèse INPL, CNRS-ENSIC, Nancy France (1992).
[6] S. Rode, N. Midoux, M. A. Latifi and A. Storck, Hydrodynamics of liquid flow in packed beds: an experimental study using electrochemical shear rate sensors, to be published in *Chem. Engn. Sci.*
[7] S. Rode, N. Midoux, M. A. Latifi and A. Storck, Hydrodynamics and liquid–solid mass transfer mechanisms in packed beds operating in cocurrent gas-liquid downflow: an experimental study using electrochemical shear rate sensors, to be published in *Chem. Engn. Sci.*
[8] B. Py, *Euromech 90 Proc.* (1970).
[9] T. J. Hanratty and J. A. Campbell, *in* 'Fluid Mechanics Measurements' (edited by R. J. Goldstein) Hemisphere, Washington (1983) p. 559.
[10] O. Wein and V. Sobolik, *Collect. Czech. Chem. Commun.* **54** (1989) 3043.
[11] P. Kaiping, *Int. J. Heat Mass Transfer* **26** (1983) 545.
[12] Z.-X. Mao and T. J. Hanratty, *ibid.* **34** (1991) 281.
[13] *Idem, Experiments in Fluids* **3** (1985) 129.
[14] S. Hiraoka, I. Yamada, H. Ikeno, H. Asano, S. Nomura, T. Okada and H. Nakamura, *J. Chem. Engng. Jpn* **14** (1981) 345.
[15] C. Deslouis, F. Huet, S. Robin and B. Tribollet, *Int. J. Heat Mass Transfer* **36** (1993) 823.